DOI: 10.61782/fa.2023.0454

forum acusticum 2023

VISCOTHERMAL EFFECTS IN DUCTS AT AUDIBLE FREQUENCIES. APPLICATION TO WIND MUSICAL INSTRUMENTS

Juliette Chabassier[1*] **Alexis Thibault**[1]
[1] MAKUTU Inria Université de Bordeaux, Talence, France

ABSTRACT

Viscous and thermal effects occur during the propagation of linear waves in a pipe. Many propagation models are used in musical acoustics, based on different assumptions that induce various model errors. The thermoviscous (or viscothermal) equations are derived from the non-linear 3D Navier-Stokes (NS) equations for a perfect gas by linearization around a uniform steady state. Analytical or numerical solutions can be proposed, after more or less deep modifications of the original system. These derived models will be summarized in a synthetic diagram specifying the assumptions performed for each one. Far from the walls, a standard 3D Helmholtz equation is valid while an effective boundary condition can replace the viscothermal "boundary layers" near the walls of the pipe. Available 1D models describe the propagation of the mean pressure on a well chosen surface and account for thermoviscous effects as a modification of the transmission line coefficients, for cylindrical and conical geometries. This work proposes an evaluation of some of these models (3D and 1D), through a quantitative estimation of model errors in relation to their domains of validity, as well as a numerical comparison for cylindrical and conical domains of propagation.

Keywords: *viscothermal boundary layers, linear acoustic wave propagation, pipe modelling, model error, input impedance*

**Corresponding author*: *juliette.chabassier@inria.fr.*

1. MODELS : GROUNDING HYPOTHESES AND VALIDITY RANGE

This work reviews thermal and viscous effects on linear wave propagation inside a pipe. It aims at understanding the ground on which are built many dissipative propagating wave models found in the musical acoustics literature, in order to quantify, as much as possible, the underlying assumptions and model errors which are performed. Details can be found in [1]. All the derived models are reviewed in Fig. 1 where a global sketch of the underlying hypotheses is proposed (see Tab. 1 for a definition of the coefficients and unknowns). The Navier-Stokes (NS) equations, which are nonlinear and expressed in the 3 dimensions of space, are the starting point of all models. Thermoviscous (or viscothermal) equations are derived from NS equations mainly after linearization and assumptions on the gas state equation, see [2]. Analytical or numerical solutions to these equations can be proposed, after modifying more of less the original system, [3–6]. It is known that the thermal and viscous effects are mainly confined near the boundaries of the pipe, in regions called "boundary layers", whose thicknesses depend on the physical coefficients and the frequency of oscillation. These thermal and viscous effects can therefore be neglected far from the boundaries (where a standard 3D Helmholtz wave equation holds), and replaced with either an effective boundary condition near the boundaries, or variable coefficients in the Helmholtz wave equation. These procedures can lead to 3D models, describing the propagation of the pressure field in all the domain or only a part of it [7–11] ; or 1D models, describing the propagation of the mean pressure across a pipe section: the most used model is the Zwikker-Kosten (Z-K) model [12–17]. Another 1D model called Webster–Lokshin (W-L) is obtained from derived 3D effective boundary condi-

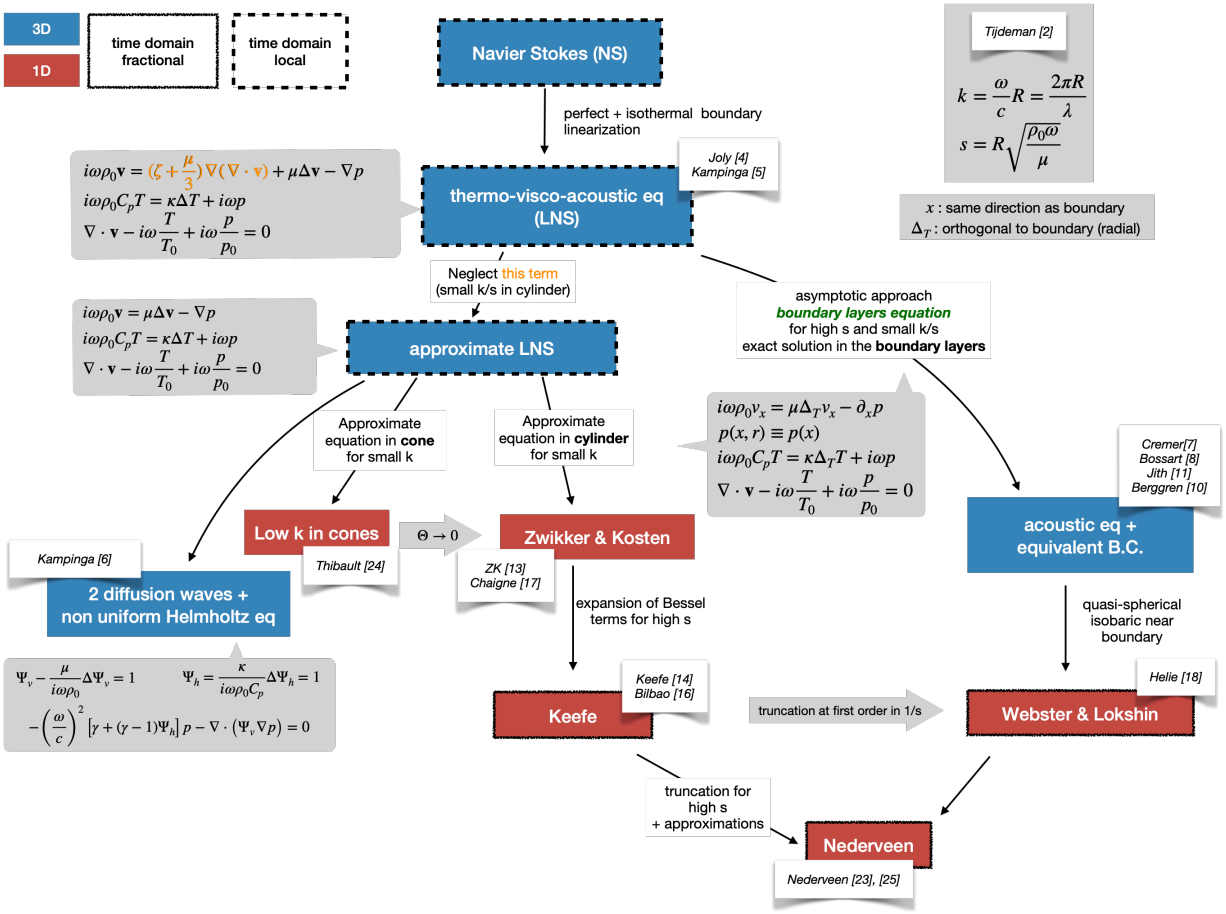

Figure 1. Derivation of some models for dissipative air columns of wind musical instruments with radius R and pulsation $\omega = 2\pi f$. The physical coefficients are defined in Tab. 1. The unknowns are the temperature T, the pressure p, the acoustic velocity $\mathbf{v}$, and the viscous and thermal potentials Ψ_v and Ψ_h for the SNLS model (bottom left).

tions, and describes the propagation of the pressure near the boundary layer [18]. These models are derived in the frequency domain. Note that in the time domain, they give rise to non-rational, non-local operators such as fractional derivatives. The use of auxiliary variables can lead to approximations which are local in time [19–22], but this is not covered here. These 1D models can also be extended to conical pipes [23–25]. All 1D models can be formulated in the same form (1) of telegrapher's equations in the frequency domain, where the expression of the lineic impedance Z_v and the shunt admittance Y_t adapts to the corresponding model. The acoustic pressure $\hat{p}$ and the acoustic volume flow $\hat{U}$ are related by

$$\frac{d\hat{p}}{dx} + Z_v(\omega, x)\hat{U} = 0, \quad \frac{d\hat{U}}{dx} + Y_t(\omega, x)\hat{p} = 0 \qquad (1)$$

where the definition of the spatial coordinate x depends on the model (axisymmetric axis, boundary curvilinear coordinate...)

From this extensive review and analysis of the models' hypotheses, their associated domains of validity are summed up in Fig. 2 in relation to the dimensionless shear number $s = R\sqrt{\rho_0\omega/\mu}$ and reduced frequency $k = R\omega/c_0$, where $\omega = 2\pi f$ is the angular frequency, R the radius of the pipe, and ρ_0 and μ are defined in Tab. 1.

Note that all the 1D models assume $k \ll 1$, i.e. that the tube radius is much smaller than the wavelength, and some models additionally assume $s \gg 1$, i.e. that the tube radius is much greater than the boundary layer thickness.

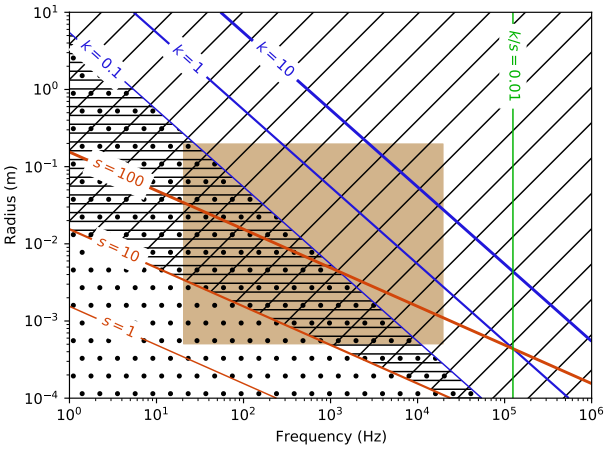

Figure 2. Expected domains of validity of the various models. The filled rectangle represents the range of pipe radii and frequencies of interest in musical acoustics. Curves of constant shear number $s = R\sqrt{\rho_0\omega/\mu}$ and reduced frequency $k = R\omega/c_0$ are displayed. The dotted region is where model (Z-K) [13] is expected to be valid, according to the hypotheses made ($k \ll 1$). Similarly, (W-L) [18] and Keefe [14] models should give accurate results in the horizontally hatched region ($k \ll 1$ and $s \gg 1$). The 3D models with effective boundary conditions [7,10] should be valid in the region with diagonal hatches. Sequential Linearized Navier Stokes model of [6] only assumes $k/s \ll 1$ hence is valid on the whole region.

2. QUANTITATIVE ASSESSMENT OF THE MODELS

An assessment of some of these 3D and 1D models allows to estimate quantitatively the model errors with respect to their domains of validity, and to compare between models for simple geometries.

2.1 Error on the complex wavenumber

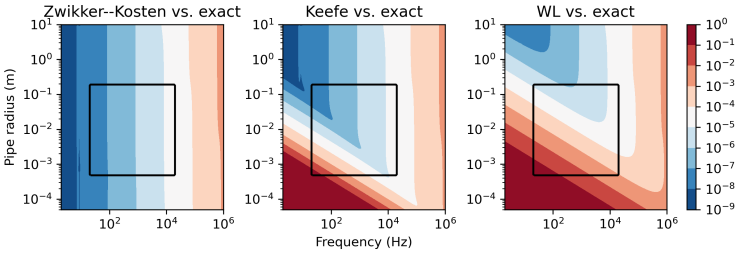

Figure 3. Relative error on the wavenumber, for models (Z-K), Keefe and (W-L), comparing them to the exact result of [12]. The black rectangle represents the range of pipe radii and frequencies of interest in musical acoustics.

First, the complex wavenumber of the different models are compared. For models of the form (1) the wavenumber is given by $\Gamma = \sqrt{Z_v Y_t}$. In Fig. 3 are displayed the relative errors on the wavenumber computed from three different models in a cylinder : (Z-K) from [13], Keefe from [14] and (W-L) from [18], with respect to the exact one of [12]. Surprisingly, (Z-K) remains valid for high k, and the error depends mostly on the ratio k/s. Since Keefe is a large-s approximation of (Z-K), it becomes invalid at low frequencies and pipe radii. As noted in [1], (W-L) can be interpreted as a large-s approximation of lower order than Keefe, thus leading to significant error at low frequencies and pipe radii. The V shape of the theoretical domains of validity of (W-L) and Keefe displayed in Fig. 2 is well recovered quantitatively in Fig. 3. An important observation is the quantitative value of these relative errors in the musical acoustics range in interest (black rectangle). It is smaller than 10^{-4} for (Z-K), but can exceed 10^{-1} with Keefe and (W-L) models when s is small.

2.2 Error on the input impedance

Second, numerical simulations will be presented and compared on canonical geometries with identical boundary conditions, so that the observed difference can only be attributed to the propagation and viscothermal model inside the pipe. The compared 3D models are based on the Helmholtz equation inside the domain, using at the wall the effective boundary conditions of [7] (Cremer BC)

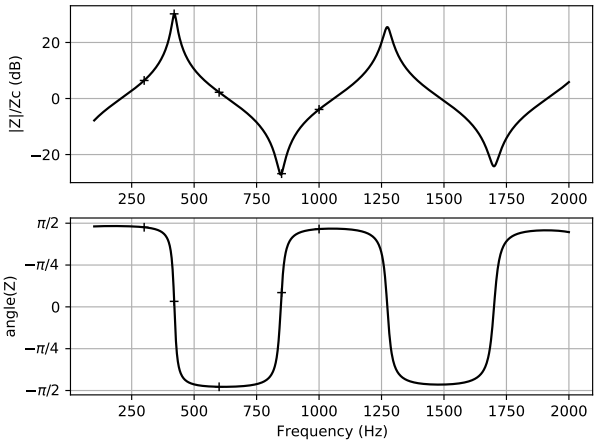

Figure 4. Input impedance of the considered perfectly open cylindrical geometry. The chosen frequencies of interest are marked with a black cross.

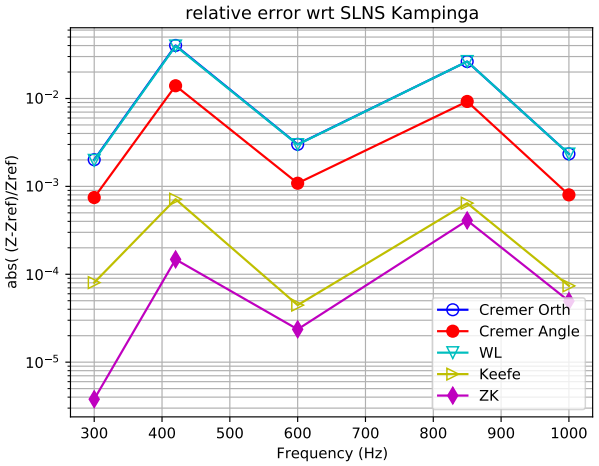

Figure 5. Relative error on the input impedance, for models Cremer BC, Cremer Angle BC, (Z-K), Keefe and (W-L), comparing them to the reference result of [6], on the cylindrical geometry.

and of [10] (Cremer Angle BC). The reference solution is computed following the sequential procedure SLNS of [6]. The compared 1D models are (Z-K) from [13], Keefe from [14], (W-L) from [18], and (S-H) or its approximation (H-R) from [24]. The 3D models are implemented in the opensource finite element library Montjoie [26] while the 1D models are implemented in the opensource library OpenWind [27]. The quantity used to compare the different simulations on a given pipe geometry is the input impedance, defined as the ratio of the fluid pressure and the volume flow through the input surface, which is a common quantity of interest in musical acoustics and can be measured experimentally [28, 29]. In the models which only compute the pressure, a correction factor is required to obtain a physically correct value of the volume flow, based on the viscous potential Ψ_v. Therefore an accurate quadrature formula must be used to finely compare 3D and 1D models, taking into account the possible curvature of the input surface. The discretisation error is controlled in the simulations [30], so that the computed difference can be attributed to the model and not to the numerical methods.

Comparisons are performed first for a cylinder of radius 4 mm and length 200 mm, with a simplified open condition ($p = 0$ at the end), at a temperature of 20°C , at different frequencies marked in Fig. 4 with black crosses on the graph of the corresponding input impedance. Fig. 5 shows the relative error on the input impedance, with respect to the reference solution obtained using the SLNS procedure of [6]. For this case, the shear number s ranges from 44 to 82 while the reduced frequency k ranges from 0.03 to 0.07. The relative model errors follow the trends predicted by model analysis. (Cremer BC) is less accurate than (Cremer Angle BC) which does not presume the angle of wavefronts with the wall. (W-L) is based on the wall impedance of (Cremer BC), indeed it is observed that both models exhibit very close error values. (Z-K) is the most accurate model, which was to be expected for the case of a cylinder. Keefe appears to be a good approximation of it, especially as the frequency (hence the shear number s) increases.

Then, comparisons are performed on a cone of input radius 4.95 mm, output radius 24.60 mm and length 61.60 mm, with a simplified open condition ($p = 0$ at the end), at a temperature of 20°C, at different frequencies marked in Fig. 6 with black crosses on the graph of the corresponding input impedance. Fig. 7 shows the relative error on the input impedance, with respect to the reference solution obtained using the SLNS procedure of [6]. For this case, the shear number s ranges from 143 to 1007 while the reduced frequency k ranges from 0.18 to 1.80. This geometry violates the underlying hypotheses of all 1D models from the simple fact that the radius R varies along the

duct, except the model (S-H) based on special functions (Legendre functions of complex order), and its approximation (H-R) which is an extension of (Z-K) where the effective radius for the losses coefficients is taken as the hydraulic radius, see [24]. To mitigate this effect, 1D computations are done using a spherical wavefront hypothesis, which is implemented as a correction of the equation coefficients, see [1]. The fact that the shear number is high for this case favors the 3D (Cremer Angle BC) model, which indeed shows small errors. The 3D (Cremer BC) model improves as the frequency increases but deteriorates at low frequencies, probably due to the erroneous presumption on the wavefronts curvatures. The 1D models (Z-K) and Keefe provide very close errors, in accordance with the fact that the shear number s is very large. Model (W-L) however cumulates the errors of (Cremer BC) and of the 1D approximation, hence displaying large errors at all frequencies. Finally, the 1D (S-H) and (H-R) models are the most precise ones, which was to be expected since they are designed for conical geometries. Note that the last point is missing for (S-H), due to difficulties to evaluate the special functions at large frequencies.

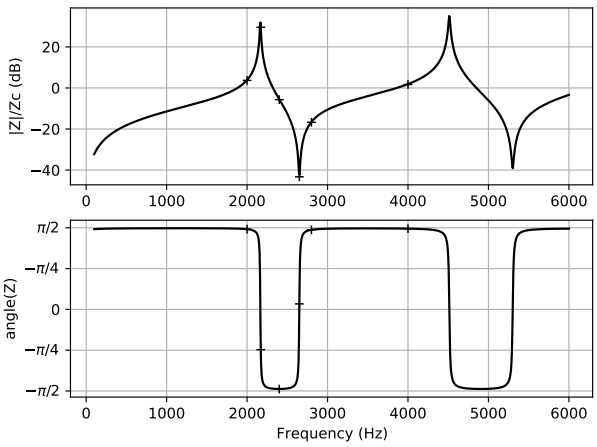

Figure 6. Input impedance of the considered perfectly open conical geometry. The chosen frequencies of interest are marked with a black cross.

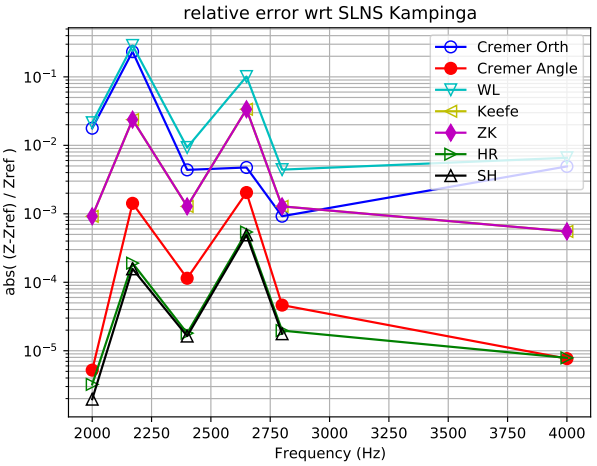

Figure 7. Relative error on the input impedance, for models (Z-K), Keefe and (W-L), comparing them to the reference result of [6], on the conical geometry.

3. CONCLUSIONS

An evaluation of several viscothermal 3D and 1D models in ducts was performed through an estimation of model errors in relation to their domains of validity. A quantitative comparison was performed on the complex wavenumber in a cylindrical geometry, and on the input impedance of a cylinder and a cone. Quantitative results corroborate qualitative predictions: it is justified to expect the model errors to decrease as the underlying assumptions of the corresponding models are respected. For most 1D models, this should be the case as the reduced frequency k is small, which occurs in thin pipes at low frequencies. For approximate 1D models as (W-L) and Keefe, the range of validity is reduced since their dissipative terms are based on the additional hypothesis that the shear number s is large. For 3D models (Cremer BC) and (Cremer Angle BC), their validity improves as the shear number s is large, which occurs in wide pipes at high frequencies. On more realistic geometries, the dimension reduction to 1D impairs the propagation effects more than the viscothermal effects, hence the comparison is dominated by the propagation model error. Further research could aim at combining improved propagation computations, for instance using the multimodal method [31], with a viscothermal model reduction.

Name	Symbol	Formula	Typical values	Unit
Static pressure	p_0		101.3	kPa
Static temperature	T_0		293.15	K
Static density	ρ_0		1.2	$\mathrm{kg \cdot m^{-1}}$
Sound velocity	c_0	$\sqrt{\gamma p_0/\rho_0}$	343.4	$\mathrm{m \cdot s^{-1}}$
Shear viscosity	μ		1.81×10^{-5}	$\mathrm{kg \cdot m^{-1} \cdot s^{-1}}$
Bulk viscosity	ζ		1.3×10^{-5}	$\mathrm{kg \cdot m^{-1} \cdot s^{-1}}$
Thermal conductivity	κ		2.57×10^{-2}	$\mathrm{J \cdot m^{-1} \cdot s^{-1}\ K^{-1}}$
Specific heat w/ constant pressure	C_p		1004	$\mathrm{J \cdot kg^{-1} \cdot K^{-1}}$
Heat capacity ratio	γ		1.402	no unit
Frequency	f		20 to 20 $\times 10^3$	Hz
Angular frequency	ω	$2\pi f$	10^2 to 10^5	$\mathrm{rad \cdot s^{-1}}$
Radius	R		10^{-3} to 10^{-1}	m
Wavelength	λ	c_0/f	2 $\times 10^{-2}$ to 20	m
Reduced frequency	k	$R\omega/c_0$	3 $\times 10^{-4}$ to.30	no unit
Shear wave number	s	$R\sqrt{\rho_0\omega/\mu}$	3 to 8000	no unit

Table 1. Notations used in this paper, from [24], for a temperature of 20°C.

4. REFERENCES

[1] J. Chabassier and A. Thibault, "Viscothermal models for wind musical instruments," Research Report RR-9356, Inria Bordeaux Sud-Ouest, Aug. 2020.

[2] H. Tijdeman, "On the propagation of sound waves in cylindrical tubes," Journal of Sound and Vibration, vol. 39, no. 1, pp. 1–33, 1975.

[3] M. Malinen, L. M, R. P, K. A, and K. L, "A finite element method for the modeling of thermo-viscous effects in acoustics," in Proceedings of the European Congress on Computational Methods in Applied Science and Engineering (ECCOMAS 2004), 2004.

[4] N. Joly, "Finite element modeling of thermoviscous acoustics on adapted anisotropic meshes: Implementation of the particle velocity and temperature variation formulation," Acta acustica united with acustica, vol. 96, no. 1, pp. 102–114, 2010.

[5] W. Kampinga, Y. H. Wijnant, and A. de Boer, "Performance of several viscothermal acoustic finite elements," Acta acustica united with Acustica, vol. 96, no. 1, pp. 115–124, 2010.

[6] W. Kampinga, Y. H. Wijnant, and A. de Boer, "An efficient finite element model for viscothermal acoustics," Acta Acustica united with Acustica, vol. 97, no. 4, pp. 618–631, 2011.

[7] L. Cremer, "On the acoustic boundary layer outside a rigid wall," Arch. Elektr. Uebertr, vol. 2, p. 235, 1948.

[8] R. Bossart, N. Joly, and M. Bruneau, "Hybrid numerical and analytical solutions for acoustic boundary problems in thermo-viscous fluids," Journal of Sound and Vibration, vol. 263, no. 1, pp. 69–84, 2003.

[9] A. Lefebvre, G. P. Scavone, and J. Kergomard, "External tonehole interactions in woodwind instruments," Acta Acustica united with Acustica, vol. 99, no. 6, pp. 975–985, 2013.

[10] M. Berggren, A. Bernland, and D. Noreland, "Acoustic boundary layers as boundary conditions," Journal of Computational Physics, vol. 371, pp. 633 – 650, 2018.

[11] J. Jith and S. Sarkar, "Boundary layer impedance model to analyse the visco-thermal acousto-elastic interactions in centrifugal compressors," Journal of Fluids and Structures, vol. 81, pp. 179–200, 2018.

[12] G. Kirchhoff, "Ueber den einfluss der wärmeleitung in einem gase auf die schallbewegung," Annalen der Physik, vol. 210, no. 6, pp. 177–193, 1868.

[13] C. Zwikker and C. W. Kosten, Sound Absorbing Materials. Elsevier Publ. Comp., 1949.

[14] D. H. Keefe, "Acoustical wave propagation in cylindrical ducts: Transmission line parameter approximations for isothermal and nonisothermal boundary conditions," The Journal of the Acoustical Society of America, vol. 75, no. 1, pp. 58–62, 1984.

[15] M. R. Stinson, "The propagation of plane sound waves in narrow and wide circular tubes, and generalization to uniform tubes of arbitrary cross-sectional shape," The Journal of the Acoustical Society of America, vol. 89, no. 2, pp. 550–558, 1991.

[16] S. Bilbao and J. Chick, "Finite difference time domain simulation for the brass instrument bore," The Journal of the Acoustical Society of America, vol. 134, no. 5, pp. 3860–3871, 2013.

[17] A. Chaigne and J. Kergomard, Acoustics of musical instruments. Springer, 2016.

[18] T. Hélie, T. Hézard, R. Mignot, and D. Matignon, "One-dimensional acoustic models of horns and comparison with measurements," Acta acustica united with Acustica, vol. 99, no. 6, pp. 960–974, 2013.

[19] T. Hélie and D. Matignon, "Diffusive representations for the analysis and simulation of flared acoustic pipes with visco-thermal losses," Mathematical Models and Methods in Applied Sciences, vol. 16, no. 04, pp. 503–536, 2006.

[20] S. Bilbao, R. Harrison, J. Kergomard, B. Lombard, and C. Vergez, "Passive models of viscothermal wave propagation in acoustic tubes," The Journal of the Acoustical Society of America, vol. 138, no. 2, pp. 555–558, 2015.

[21] S. Bilbao and R. Harrison, "Passive time-domain numerical models of viscothermal wave propagation in acoustic tubes of variable cross section," The Journal of the Acoustical Society of America, vol. 140, no. 1, pp. 728–740, 2016.

[22] A. Thibault and J. Chabassier, "Dissipative time-domain one-dimensional model for viscothermal acoustic propagation in wind instruments," The Journal of the Acoustical Society of America, vol. 150, no. 2, pp. 1165–1175, 2021.

[23] C. J. Nederveen, Acoustical aspects of woodwind instruments. Frits Knuf, 1969.

[24] A. Thibault, J. Chabassier, H. Boutin, and T. Hélie, "Transmission line coefficients for viscothermal acoustics in conical tubes," Journal of Sound and Vibration, vol. 543, p. 117355, 2023.

[25] T. Grothe, J. Baumgart, and C. J. Nederveen, "A transfer matrix for the input impedance of weakly tapered cones as of wind instruments," arXiv preprint arXiv:2303.12750, 2023.

[26] Marc Duruflé, "Montjoie." `https://www.math.u-bordeaux.fr/~durufle/montjoie/index.php`.

[27] Chabassier, Juliette and Ernoult, Augustin and Tournemenne, Robin and Thibault, Alexis and Geber, Olivier and Van Baarsel, Tobias and Castera, Guillaume, "Openwind : Python library assisting instrument makers." `https://openwind.inria.fr`.

[28] V. Gibiat and F. Laloë, "Acoustical impedance measurements by the two-microphone-three-calibration (tmtc) method," The Journal of the Acoustical Society of America, vol. 88, no. 6, pp. 2533–2545, 1990.

[29] J.-P. Dalmont and J. C. Le Roux, "A new impedance sensor for wind instruments," The journal of the Acoustical Society of America, vol. 123, no. 5, pp. 3014–3014, 2008.

[30] R. Tournemenne and J. Chabassier, "A comparison of a one-dimensional finite element method and the transfer matrix method for the computation of wind music instrument impedance," Acta Acustica united with Acustica, vol. 105, no. 5, pp. 838–849, 2019.

[31] T. Guennoc, J.-B. Doc, and S. Félix, "Improved multimodal formulation of the wave propagation in a 3d waveguide with varying cross-section and curvature," The Journal of the Acoustical Society of America, vol. 149, no. 1, pp. 476–486, 2021.